Title

Interaction forces and membrane charge tunability: Oleic acid containing membranes in different pH conditions

Journal

Biochimica et Biophysica Acta (BBA) - Biomembranes, 1859(2)

ISSN

0005-2736

Authors

Kurniawan, James
Suga, Keishi
Kuhl, Tonya L

Publication Date

2017-02-01

DOI

10.1016/j.bbamem.2016.11.001

Peer reviewed

Biochimica et Biophysica Acta 1859 (2017) 211–217

Contents lists available at ScienceDirect

Biochimica et Biophysica Acta

journal homepage: www.elsevier.com/locate/bbamem

Interaction forces and membrane charge tunability: Oleic acid containing membranes in different pH conditions

James Kurniawan [a], Keishi Suga [b,*], Tonya L. Kuhl [a,c,**]

[a] Department of Chemical Engineering, University of California Davis, 95616, USA
[b] Division of Chemical Engineering, Graduate School of Engineering Science, Osaka University, 1-3 Machikaneyamacho, Toyonaka, Osaka 560-8531, Japan
[c] Department of Biomedical Engineering, University of California Davis, 95616, USA

ARTICLE INFO

Article history:
Received 25 July 2016
Received in revised form 27 October 2016
Accepted 2 November 2016
Available online 04 November 2016

Keywords:
Oleic acid
DPPC
Supported lipid bilayer
Isotherm
Protonation
SFA

ABSTRACT

Oleic acid is known to interact with saturated lipid molecules and increase the fluidity of gel phase lipid membranes. In this work, the thermodynamic properties of mixed monolayers of 1,2-dipalmitoyl-*sn*-glycero-3-phosphocholine (DPPC) and oleic acid at the air-water interface were determined using Langmuir isotherms. The isotherm study revealed an attractive interaction between oleic acid and DPPC. The incorporation of oleic acid also monotonically decreased the elastic modulus of the monolayer indicative of higher fluidity with increasing oleic acid content. Using the surface force apparatus, intermembrane force–distance profiles were obtained for substrate supported DPPC membranes containing 30 mol% oleic acid at pH 5.8 and 7.4. Three different preparation conditions resulted in distinct force profiles. Membranes prepared in pH 5.8 subphase had a low number of nanoscopic defects ≤1% and an adhesion magnitude of ~0.6 mN/m. A slightly higher defect density of 1–4% was found for membranes prepared in a physiological pH 7.4 subphase. The presence of the exposed hydrophobic moieties resulted in a higher adhesion magnitude of 2.9 mN/m. Importantly, at pH 7.4, some oleic acid deprotonates resulting in a long-range electrostatic repulsion. Even though oleic acid increased the DPPC bilayer fluidity and the number of defects, no membrane restructuring was observed indicating that the system maintained a stable configuration.

1. Introduction

Biologically occurring fatty acids have been extensively studied due to their strong link to numerous health benefits [1,2]. Fatty acids, which are found in foods such as fruits, seeds, nuts, vegetable oils, animal fats, and fish oils, can be categorized into saturated, monounsaturated, polyunsaturated, and *trans* fats. Both saturated and *trans* fatty acids has been shown to increase the risk of cardiovascular diseases [3–6]. In contrast, unsaturated fatty acids have been shown to have a potentially therapeutic benefit for patients with type-2 diabetes [7], dementia [8], cystic fibrosis [9], and arguably to reduce the risk of coronary heart diseases [10–13]. In particular, polyunsaturated fatty acids (PUFAs) such as α-linolenic acid (omega-3) and linoleic acid (omega-6) have received the most attention as humans cannot synthesize either of these molecules. As a result, the importance of the monounsaturated fatty acids (MUFAs) has been somewhat overshadowed.

Oleic acid is an example of monounsaturated omega-9 free fatty acid and is a major constituent in vegetable oil derived from olive, rapeseed, and sesame seeds. Free fatty acids, such as oleic acid can intercalate into lipid membranes and alter their physicochemical properties [14,15]. Specifically, due to the kinked cis-double bond structure, oleic acid has been shown to alter the structure, fluidity, and permeability of saturated phospholipid monolayers and bilayers [16–18]. Based on monolayer studies, Gonçalves et al. reported attractive lateral interactions between oleic acid and DPPC based on a decrease in the area per molecule in their mixtures at the air-water interface [19]. Thermodynamic analysis using differential scanning calorimetry (DSC) revealed the melting temperature of DPPC-oleic acid mixtures decreased up to ~50 mol% oleic acid content [20]. Additional measurements indicated that the fluidity of DPPC membranes concomitantly increased with the presence of oleic acid [21]. The miscibility of oleic acid in DPPC membranes and fluidization of the membrane was corroborated by molecular dynamics simulation studies performed by Cerezo and coworkers [22]. Their simulations also found an increase in lateral diffusivity in the mixed system and enhancement in membrane permeability. The interaction between oleic acid and DPPC molecules is also likely to affect the deprotonation of the oleic acid's carboxyl headgroup. The pKa of an isolated carboxyl group in water is ~4.8 [23], while the apparent pKa of oleic acid's carboxyl headgroup tends to be higher depending on the type of co-

* Correspondence to: K. Suga, Division of Chemical Engineering, Osaka University, Osaka 560-8531, Japan.
** Correspondence to: T.L. Kuhl, Department of Chemical Engineering, University of California Davis, 95616, USA.
E-mail addresses: keishi.suga@cheng.es.osaka-u.ac.jp (K. Suga), tlkuhl@ucdavis.edu (T.L. Kuhl).

http://dx.doi.org/10.1016/j.bbamem.2016.11.001
0005-2736/

existing molecules in the mixture and structure of the assembly (*i.e.*, pKa of ~6.1 in the hexagonal phase of oleic acid and monoolein mixtures [24]; pKa of ~6.5 in 4:6 oleic acid-DPPE vesicles [25]; pKa of ~8.0–8.5 in pure oleic acid vesicles [23]; and, an even higher pKa of ~9.85 for oleic acid monolayers at air-water interface [26]). The deprotonation of oleic acid in the system consequently alters molecular level lateral interactions and phase behavior of the mixture [23,27]. Likewise, deprotonation would significantly impact the interaction between membranes and oleic acid can be used to induce pH-dependent membrane fusion or membrane repulsion in model systems [25,28,29]. The ability to alter the charge of oleic acid through pH enables switching between attractive, null and repulsive electrostatic interactions in membranes. For example, positively charged vesicles will spontaneously fuse with negatively charged vesicles containing oleic acid under alkaline conditions. Beyond the ability to tailor the charge of membranes containing oleic acid through pH, incorporation of oleic acid may alter membrane structure, fluidity, permeability as well as water of hydration and entropic motion such as membrane protrusions and undulations.

In this work, the lateral interaction between oleic acid and DPPC molecules in monolayers was examined using Langmuir isotherms at the air-water interface as a function of oleic acid concentration. The isotherm studies were used to determine the Gibbs free energy of mixing and changes in monolayer compressibility, which are indicative of constituent molecule interactions and membrane fluidity. The interaction forces between 7:3 DPPC-oleic acid membranes were investigated at different pH conditions using the surface force apparatus (SFA) technique [30]. Force profiles were measured and compared at physiological pH 7.4, where full deprotonation is expected, and at pH 5.8. The force profile measurements also enabled the membrane thickness, adhesive minimum and surface charge density to be directly determined.

2. Materials and methods

2.1. Chemicals

1,2-Dihexadecanoyl-*sn*-glycero-3-phosphoethanolamine (DPPE, melting point, T_M = 63 °C) and 1,2-dipalmitoyl-*sn*-glycero-3-phosphocholine (DPPC, T_M = 41 °C) were purchased from Avanti Polar Lipids, Inc. (Alabaster, AL) and used as received. Oleic acid (*cis*-9-octadecanoic acid, T_M = 13–14 °C), monosodium phosphate (NaH_2PO_4 99.999%), disodium phosphate (Na_2HPO_4 99.95%) and sodium nitrate ($NaNO_3$ 99.995%) were purchased from Sigma-Aldrich (St. Louis, MO). Water was purified with a MilliQ gradient water purification system to a resistivity of 18 MΩ·cm.

2.2. Isotherm of DPPC-oleic acid at the air-water interface

Pressure-area isotherms (Π-*A*) of various DPPC-oleic acid mixtures were obtained on a pure water subphase at 25 °C under an inert environment, depleted of oxygen, which inhibits oxidation of carbon-carbon double bonds. The isotherms were obtained without prior compression cycles with a compression ratio of about 17 cm^2/min, which corresponds to a compression rate of 2–3 $Å^2$ per molecule per min. The lateral interaction between DPPC and oleic acid molecules such as the monolayer elastic modulus, C_s^{-1}, excess area, A_{ex} and Gibbs excess free energy of mixing, ΔG_{mix} were calculated from the isotherm data. The elastic modulus is defined as the product of the average area per molecule (A) and the slope of the Π-*A* isotherm at a specific surface pressure.

$$C_s^{-1} = -A\frac{d\Pi}{dA} \tag{1}$$

Excess area was calculated using the area per molecule data from the pure component and mixture isotherms given by

$$A_{ex} = A_{12} - (x_1A_1 + x_2A_2) \tag{2}$$

where A_{12}, A_1, A_2 are area per molecule of the DPPC-oleic acid mixture, DPPC, and oleic acid, respectively, and x_1 and x_2 are molar fractions of DPPC and oleic acid, respectively. The total Gibbs excess free energy of mixing is defined as

$$\Delta G_{mix} = \Delta G_{ex} + \Delta G_{ideal} \tag{3}$$

where the excess Gibbs free energy, ΔG_{ex}, was obtained by integrating A_{ex} with respect to the surface pressure, $\Delta G_{ex} = \int A_{ex} d\Pi$, and the ideal Gibbs free energy of mixing was calculated by

$$\Delta G_{ideal} = kT(x_1 \ln(x_1) + x_2 \ln(x_2)) \tag{4}$$

where k is the Boltzmann constant and T is absolute temperature.

2.3. Membrane preparation

Mica substrate supported lipid membranes were used in SFA and AFM studies. The membranes were constructed using Langmuir-Blodgett (LB) deposition (Nima Coventry, U.K.). The inner monolayer for all the experiments was DPPE deposited using Langmuir-Blodgett (LB) method at 45 mN/m and dipping speed of 1 mm/min with a MilliQ water subphase (pH = 5.8). Previous studies have shown that LB deposited DPPE forms an almost defect free, robust and strongly physisorbed monolayer on mica with transfer ratios of 0.997 ± 0.004 [31] and a thickness of 2.56 ± 0.05 nm under these conditions [32]. As the underlying mica support is negatively charged, this near perfect DPPE inner monolayer minimizes any charge originating from the substrate. In addition, the tight packing and stability of the gel phase DPPE inner monolayer minimizes molecular exchange between the two leaflets. The outer monolayer was 7:3 DPPC-oleic acid LB deposited at 35 mN/m and dipping speed of 1 mm/min on MilliQ water (pH = 5.8) or 0.5 mM phosphate buffer (pH = 7.4) subphase. The average molecular areas for the 7:3 DPPC-oleic acid outer monolayer were 34.2 ± 1.0 $Å^2$ at pH 5.8 and 33.7 ± 1.5 $Å^2$ at pH 7.4.

2.4. Surface force apparatus measurements (SFA)

The SFA technique has been used extensively to measure the interaction forces between surfaces and details of the technique can be found in the following references [30–34]. Based on multiple-beam interferometry (MBI) [35], the SFA provides a definitive reference for the surface separation (±0.2 nm in this work). Briefly, one of the membrane coated mica surfaces was mounted on a fixed stage and the other on a vertically displaceable double cantilever spring of known stiffness (2.6×10^5 mN/m). The back of the mica substrates was coated with a 55 nm thick, evaporated silver layer. The silver layer on each disk partially transmits light directed normally through the surfaces which constructively interferes producing fringes of equal chromatic order (FECO). The distances between the surfaces can be measured by observation of the position and displacement of FECO peak wavelengths within a spectrometer. A custom automated SFA Mark-II was used for data collection. The system enables constant and/or variable surface displacements via a computer-controlled motor system. A sensitive CCD camera (Princeton SPEC-10:2K Roper Scientific, Trenton, NJ) was interfaced with the spectrometer and computer acquisition system to allow automated FECO wavelength determination.

After membrane deposition, the surfaces were transferred and mounted in the SFA. SFA force profile measurements were done in either 0.5 mM $NaNO_3$ solution at pH 5.8 or 0.5 mM phosphate buffer at pH 7.4. In both cases the solution was saturated with lipids to minimize desorption from the surface during the course of the

measurements. After the surfaces were mounted, the SFA was placed in a temperature-controlled room at 25.0 °C for at least two hours to allow equilibration. The membrane thickness was determined using the FECO wavelength shift from membrane contact relative to bare mica substrates after completing each experiment. As the membranes were asymmetric with inner leaflets of DPPE and outer leaflets of DPPC-oleic acid mixtures, we treated the two outer leaflets, which we are primarily interested in, as an equivalent membrane of the mixture composition. Force profiles shown in the results section are representative force-distance profiles of three independent experiments at three different experimental conditions. The experimental conditions were (i) both the inner and outer monolayers LB deposited on MilliQ water subphase at pH 5.8 and the force profiles measured in 0.5 mM $NaNO_3$ solution at pH 5.8; (ii) membrane deposited on MilliQ water subphase at pH 5.8, but with the force profiles measured in 0.5 mM phosphate buffer at pH 7.4; (iii) outer membrane leaflet deposition and force measured in 0.5 mM phosphate buffer at pH 7.4. At least five repeatable force measurements were taken for each experimental condition and the reported error propagation in the results section was based on the average of the five force runs for each condition. Force-distance profiles which include multiple data sets for each experimental condition are included in the Supplementary material.

2.5. Atomic force microscopy (AFM)

AFM images were acquired using a MFP3D-SA system (Asylum Research, Santa Barbara, CA). A silicon cantilever (model MSNL-10, Bruker, Santa Barbara, CA) with force constant of 0.6 N/m was used for imaging. All the images were acquired in contact mode with a force of 12 nN. AFM images were analyzed using Gwyddion Version 2.31 (http://gwyddion.net/).

3. Results

3.1. Monolayer properties of DPPC-oleic acid mixtures

Pressure-area (Π-*A*) isotherms of DPPC-oleic acid mixtures were measured on a pure water subphase (Fig. 1A). In general, the area per molecule at each pressure decreased with increasing oleic acid molar ratio [19]. Isotherm data were used to calculate the elastic moduli and excess Gibbs free energy of mixing of the mixtures (Eq. (1)). The elastic moduli of pure DPPC plateaued at a surface pressure range of 28–37 mN/m (Fig. 1B). Due to the noise in the data, a moving average value was used to obtain the average elastic moduli. As shown in Fig. 1C, a trend of decreasing elastic moduli with increasing oleic acid was observed. To estimate the miscibility of oleic acid in DPPC, the excess Gibbs free energy of mixing was determined (Eq. (3)) [36,37]. The excess Gibbs free energy of mixing values was negative for all DPPC-oleic acid mixtures which indicates a favorable interaction between DPPC and oleic acid (Fig. 1D). It has been reported that hydrogen bonding between oleic acid molecules and DPPC could alter the apparent pKa value of oleic acid [38]. To further elucidate the impact of lateral interactions and embedding of oleic acid in a phospholipids membrane on deprotonation, membrane thickness, and adhesion, the interaction force profiles between 7:3 DPPC-oleic acid membranes were directly measured with an SFA under the various deposition and solution conditions listed previously.

3.2. Force–distance profile of 7:3 DPPC-oleic acid at different pH

Fig. 2 shows the measured force profiles between opposing membranes with 7:3 DPPC-oleic acid as the outer monolayer at three different experimental conditions. When both the inner and outer monolayers were LB deposited on MilliQ water subphase at pH 5.8 and the force profiles measured in 0.5 mM $NaNO_3$ solution at pH 5.8, the thickness of the equivalent of 7:3 DPPC-oleic acid membrane was 7.8 ± 0.2 nm. This equivalent thickness is defined as the thickness of the two outer monolayers including the water of hydration between the bilayers. The magnitude of adhesion between the membranes was 0.6 ± 0.1 mN/m and no electrostatic repulsion was observed. The lack of electrostatic repulsion is consistent with a very low-degree of deprotonated oleic acid at pH of 5.8 (pKa of oleic acid >6.1) [24].

Using the same membrane preparation method (where the membrane was LB deposited in MilliQ water at pH 5.8), but force profile measurements were done in 0.5 mM pH 7.4 phosphate buffer subphase, the thickness of the equivalent 7:3 DPPC-oleic acid membrane was 7.4 ± 0.2 nm. The force profiles clearly showed a long-range electrostatic repulsion with decay length consistent with the electrolyte concentration and a short-range attraction. The electrostatic contribution was fitted using the non-linearized Poisson–Boltzmann equation with constant charge approximation. A constant surface charge density of 1.3 ± 0.3 mC/m^2 or surface potential of -25 ± 3 mV was obtained with the origin of charge at the membrane surface. The thickness and adhesion of the equivalent 7:3 DPPC-oleic acid membranes at pH 5.8 and 7.4 were similar due to the identical deposition conditions. As the electrostatic and van der Waals attraction should be additive, the electrostatic interaction was subtracted from the total force profile to extract the attractive contribution to the membrane-membrane interaction. After removing the electrostatic contribution, the membrane adhesion magnitude was 0.7 ± 0.1 mN/m (Fig. 2C).

When both the deposition of the outer monolayer and the force measurement were done in 0.5 mM pH 7.4 phosphate buffer, a significantly thinner 7:3 DPPC-oleic acid membrane with equivalent thickness of 6.0 ± 0.2 nm was obtained. Again, because of the higher pH, the oleic acid molecules were partially deprotonated resulting in a long-range electrostatic repulsion. The surface charge density was slightly higher than the case of depositing the membrane at pH 5.8 and measuring the force profiles at pH 7.4. At pH 7.4 conditions, a constant surface charge density of 2.1 ± 0.4 mC/m^2 or surface potential of -38 ± 6 mV was obtained. After subtracting the electrostatic contribution, the magnitude of the membrane adhesion was substantially greater at 2.9 ± 0.1 mN/m (Fig. 2C). Results for the SFA measurements are summarized in Table 1.

In order to corroborate the resulting force profiles with membrane structure under different preparation conditions, high-resolution AFM topography scans were done on LB deposited 7:3 DPPC-oleic acid membranes at pH 5.8 and 7.4 (Fig. 3). No phase separated domains were observed, but the AFM scans revealed topological membrane defects that extended down to the inner DPPE monolayer in both cases. When 7:3 DPPC-oleic acid was prepared in MilliQ water at pH 5.8, more uniform, well-packed membranes were obtained. Based on image analysis of four independent samples with at least five different regions scanned per sample, the average defect depth was 2.0 ± 0.7 nm with coverage area between 0 and 1% of the supported membrane [39]. In one case, multiple membrane spanning holes that penetrated the DPPE inner monolayer were detected (Fig. 3). When the outer membrane leaflet was deposited from an 0.5 mM phosphate buffer at pH 7.4, significantly more topological defects were found. Based on analysis of two independent samples with at least five different regions scanned per sample, the surface coverage of the defects ranged between 1 and 4% [39] with an average defect depth of 2.3 ± 0.8 nm.

4. Discussion

4.1. Langmuir monolayer analysis of DPPC-oleic acid lateral interaction

Isotherms of various DPPC-oleic acid mixtures revealed that the fluid to gel phase transition of DPPC was maintained in DPPC-oleic acid mixtures, indicating that DPPC still formed the continuous phase. The absence of phase separation in the 7:3 DPPC-oleic acid membranes was corroborated by the high resolution AFM topography scan

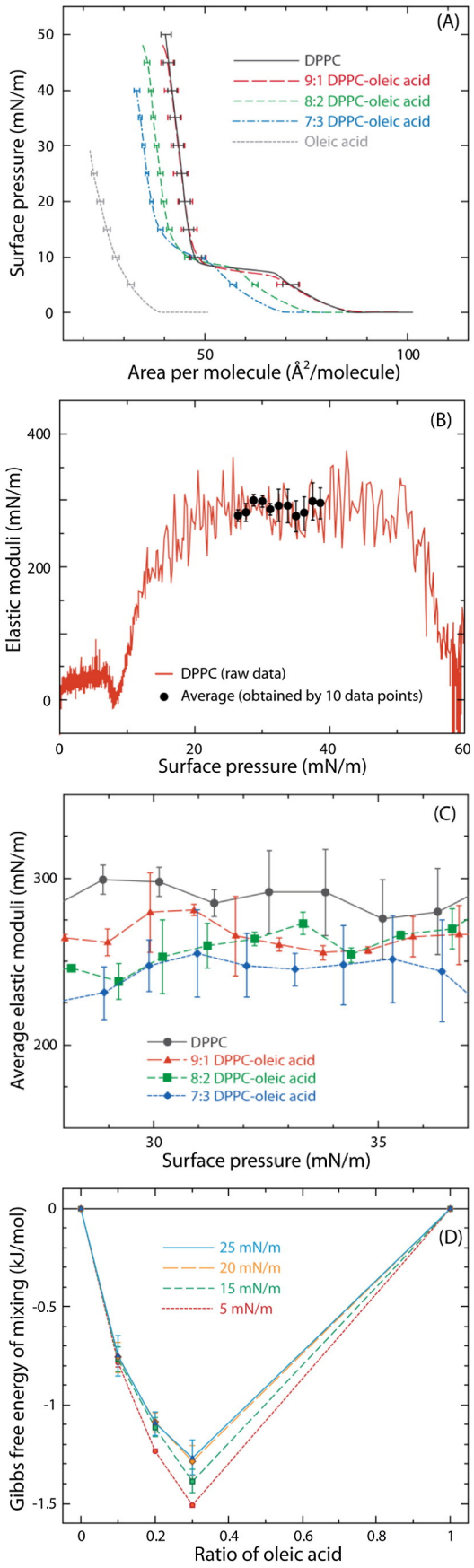

(Fig. 3). The isotherm of the DPPC-oleic acid mixtures also indicated stabilization of oleic acid by the lateral interaction with DPPC lipids. For all oleic acid concentrations studied, the DPPC-oleic acid monolayer was able to compress beyond the collapse pressure of a pure oleic acid monolayer (~30 mN/m) and there was no indication of oleic acid squeezing out from the air-water interface at a surface pressure of 35 mN/m. These results demonstrate that DPPC and oleic acid are miscible with each other, and the interaction between DPPC and oleic acid molecules is favorable under the experimental conditions studied. Additionally, one of the roles of unsaturated fatty acid in membranes is to destabilize ordered structures such as raft domains. Onuki et al. reported that 30% of oleic acid significantly fluidized DPPC membranes, resulting in a decrease of detergent-insolubility [40]. The monolayer elastic modulus is a measure of the membrane stiffness and correlated to the fluidity of the membrane. The experimental data showed that incorporation of oleic acid into DPPC monolayers decreased the film stiffness (Fig. 1C). Although the differences of elastic modulus in DPPC and DPPC-oleic acid mixture were small, the averaged values show a decreasing trend with increasing oleic acid in the monolayer. Thus, incorporation of oleic acid decreases the stiffness of DPPC monolayers and correspondingly increases monolayer fluidity [21].

4.2. Adhesion between 7:3 DPPC-oleic membranes

When the membranes were deposited in MilliQ water at pH 5.8, the effective membrane adhesion due to attractive van der Waals interactions was consistent and matched well with the measured adhesion between pure fluid phase PC membranes of 0.6 ± 0.1 mN/m reported by Marra and Israelachvili [34]. In addition, the fluidization effect of oleic acid incorporation into DPPC membrane observed by Langmuir monolayer analysis is consistent with the lower adhesion compared to gel phase DPPC [34]. However, the mixed oleic acid-DPPC membrane was thicker at 7.4–7.8 nm compared to the thickness of gel phase DPPC presumably deposited on DPPE of 5.5 ± 0.3 nm [34] and our own measurements of DPPC on DPPE membrane thickness of 6.0 ± 0.2 nm using the SFA. Similar values were obtained from X-ray reflectivity measurements of supported DPPC membranes on quartz [39]. Possible, even coexisting, reasons for the increase in apparent membrane thickness include (i) a larger hydration shell of charged oleic acid in the DPPC membrane, (ii) greater protrusions of the single acyl chain fatty acid out of the membrane plane and/or (iii) a decrease in tilt of the DPPC lipids from surface normal. Further studies such as high-resolution X-ray scattering and NMR hydration studies could help quantify these different contributions. In contrast, the higher level of defects on the 7:3 DPPC-oleic acid membranes deposited at pH 7.4 led to a thinner membrane and significantly higher adhesion. The difference in the adhesion magnitude of about 2 mN/m was attributed to hydrophobic attraction due to the higher amount of exposed inner monolayer acyl chains or hydrophobic moieties in the contact regions [41].

4.3. Dissociation of oleic acid in mixed 7:3 DPPC-oleic acid membranes

Fatty acid molecules self-assemble into micelles, vesicles, and other closed structures in aqueous media. Their deprotonation depends on the surrounding pH and the type of any associated lipids or molecules in the assembled structure. Previous studies have shown that the apparent pKa of oleic acid in different surfactant and lipid mixtures ranges from 6.0 to 9.5. For example, the pKa of pure oleic acid vesicles is 8.0–

Fig. 1. (A) Π-*A* isotherms of DPPC-oleic acid on MilliQ water. (B) Elastic moduli (C_s^{-1}) as a function of surface pressure during compression of DPPC monolayers. Line indicates raw data while the circles with error bars are the moving average of 10 data points. (C) Comparison of average elastic modulus values over the surface pressure range of 28–37 mN/m. (D) Gibbs free energy of mixing (ΔG_{mix}) of DPPC-oleic acid membranes at various surface pressures. All measurements were carried out at room temperature.

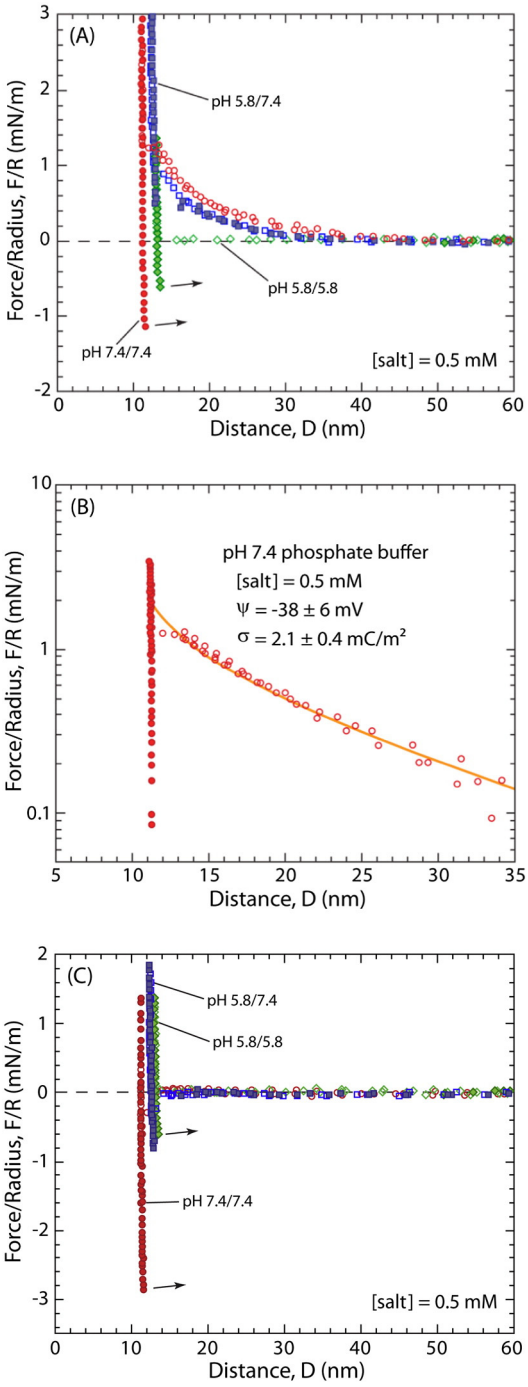

Fig. 2. (A) Force–distance profiles between 7:3 DPPC-oleic acid membranes under three different experimental conditions. The pH during the membrane deposition is shown as the first value and the pH during force profile measurements is shown as the second value, where diamonds pH 5.8/5.8, squares pH 5.8/7.4, and circles pH 7.4/7.4. Open and filled symbols indicate approach and separation respectively. (B) Semi-logarithmic plot of the force profile of 7:3 DPPC-oleic acid membranes prepared and measured in 0.5 mM pH 7.4 phosphate buffer (pH 7.4/7.4). The solid line is the fitted electrostatic contribution with the origin of charge at the membrane surface. $D = 0$ is defined as the contact between bare mica–mica surfaces. (C) Subtraction of the electrostatic contribution and corresponding attractive contribution to the force profile.

9.5 [27,42,43]. While when mixed with monoolein, the pKa was 6.0–7.0 [24]. A similar pKa of 6.5 was found for 4:6 oleic acid-DPPE vesicles [25].

The force profile measurements and determination of the surface charge density of 7:3 DPPC-oleic acid SLBs under various pH conditions enable the deprotonation level of oleic acid in DPPC membranes to be extracted precisely. At pH 5.8, no electrostatic repulsion was measured

Table 1
Summary of SFA results at three different experimental conditions.

pH during deposition	pH for force run	Equivalent thickness (nm)[a]	σ (mC/m^2)	Ψ (mV)	$\lvert F_{ad}/R\rvert_{VdW}$ (mN/m)
5.8	5.8	7.8 ± 0.2	N/A	N/A	0.6 ± 0.1
5.8	7.4	7.4 ± 0.2	−1.3 ± 0.3	−25 ± 3	0.7 ± 0.1
7.4	7.4	6.0 ± 0.2	−2.1 ± 0.4	−38 ± 6	2.9 ± 0.1

[a] The equivalent thickness is the thickness of the two outer monolayers including their hydration layer.

indicating that oleic acid does not dissociate (deprotonate) under these conditions. At pH 7.4, regardless of the deposition being at pH 5.8 or 7.4, a long-range electrostatic repulsion was observed. The electrostatic repulsion is clearly due to partially dissociated (negatively charged) oleic acid molecules in the membrane. The level of charge was lower in the case of the mixed monolayer being deposited from a water subphase (pH 5.8) than in a buffered subphase (pH 7.4). Under the former conditions, a constant surface charge density of 1.3 mC/m^2 was obtained, which corresponds to 0.9% of the oleic acid molecules dissociating. The degree of oleic acid dissociation was calculated using average the area per molecule of 34.2 Å^2 at 35 mN/m (see Supplementary material). The apparent pKa value of oleic acid in the 7:3 DPPC-oleic acid membrane was estimated to be pKa = 9.4 ± 0.2 using the Henderson-Hasselbalch equation. In comparison, when the 7:3 DPPC-oleic acid outer layer was deposited on a pH 7.4 subphase, a higher surface charge density of 2.1 mC/m^2 was measured. The deprotonation degree of oleic acid under this experimental condition corresponds to 1.5% deprotonation, and an apparent pKa value of 9.2 ± 0.1. These apparent pKa values should be an upper bound as the pH of the environment precisely at the membrane surface and oleic acid molecules is slightly reduced by the stationary buffer layer above the membrane. Based on previous work by Kramer et al., the pH at the membrane surface was estimated to be 7.0 [44] and thus the lower bound of the apparent pKa of oleic acid would be 0.4 pH units lower than the upper bound values provided above.

The pKa of isolated carboxylic groups in water is much lower at 4.8 [23]. Clearly, the fatty acid chain length and structure of the self-assembled system are key factors in shifting the apparent pKa to higher (more alkaline) values [45]. In particular, our work demonstrates that the apparent pKa of oleic acid in 7:3 DPPC-oleic acid ranges between 8.8 and 9.4 ± 0.2. By their very definition, self-assembled structures of amphiphilic molecules require close proximity of the low dielectric environment of the acyl region and hydrophilic potentially charged headgroup region. Low dielectric media greatly reduce charge dissociation and this is the main reason for the low deprotonation of oleic acid in mixed DPPC membranes. In addition, the measured negative excess Gibbs free energy of mixing, ΔG_{mix}, for mixed DPPC and oleic acid monolayers demonstrates favorable interactions between DPPC and oleic acid on a pure water subphase [19]. Favorable lateral association between and with lipid molecules and surfactants is also consistent with inhibition of oleic acid deprotonation.

The results further demonstrate that deprotonation of oleic acid in mixed monolayers decreases the quality of monolayer transfer during LB deposition. The 7:3 DPPC-oleic acid membrane prepared in pH 7.4 was thinner due to more defects and had a higher surface charge density than the membrane prepared in pH 5.8. The thinner membrane and presence of defects lower the lateral packing density and thus increased the spacing between headgroups. The lower lateral packing density enables greater deprotonation primarily due to increasing the effective dielectric in the headgroup region. The change in packing would also result in a larger spacing between molecules further aiding deprotonation as well as changes in the lateral interactions between headgroups such as hydrogen bond formation.

The alteration in the membrane surface charge density in conjunction with the increase in membrane fluidity should reduce the barrier

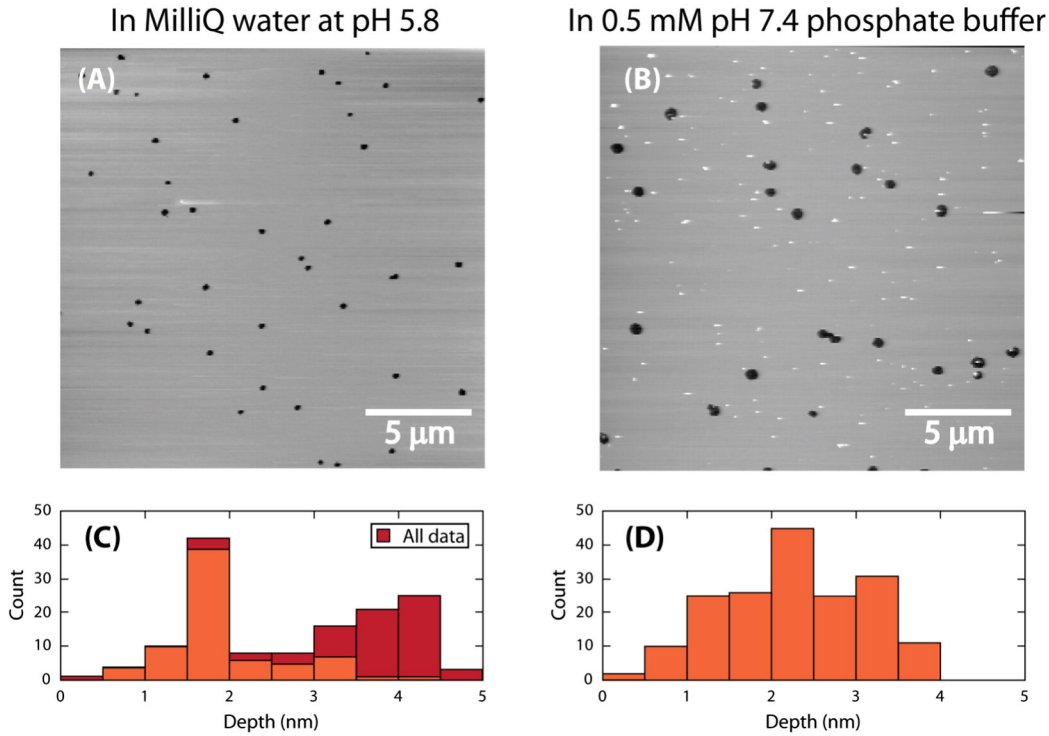

Fig. 3. 20 × 20 μm AFM scan of 7:3 DPPC-oleic acid on DPPE membrane LB deposited on mica in pH 5.8 MilliQ water [A] and in 0.5 mM pH 7.4 phosphate buffer [B]. [C] Histogram of the defect depth for 7:3 DPPC-oleic acid on DPPE membrane in pH 5.8 MilliQ water (orange) and histogram of defects + holes that reached the underlying mica substrate found in one scan (red). [D] Histogram of the defect depth for 7:3 DPPC-oleic acid on DPPE membrane in 0.5 mM pH 7.4 phosphate buffer. The histograms were constructed based on 2–4 independent samples with at least 5 different regions scanned per sample yielding 10–20 analyzed images. The average depths and defect density area were statistically analyzed with error bars as standard deviation: in pure water, depth = 2.0 ± 0.7 nm, defect area = 0.6 ± 0.4%; in pH 7.4 buffer, depth = 2.3 ± 0.8 nm, defect area = 1.5 ± 0.7%.

function of the membrane towards external molecules, which would enhance insertion of external molecules into the membrane and increase cellular uptake efficiency of drugs. As membrane properties can be a key factor in membrane-associated interactions [46], these changes in membrane properties could also affect the localization of membrane associated enzymes or proteins and thereby impact metabolic pathways. For example, oleic acid has been shown to modify G-protein-mediated signaling cascades that regulate adenylyl cyclase and phospholipase C [47]. Lastly, the properties of oleic acid are also modified by membrane composition and structure leading to changes in the apparent pKa. These findings enhance our understanding of the potential biological significance of free fatty acids.

5. Conclusion

Membrane interactions and the deprotonation behavior of oleic acid in a DPPC membrane at physiological pH were determined in this work. The interaction between 7:3 DPPC-oleic acid membranes was repulsive at pH 7.4, due to electrostatic interactions consistent with pH induced dissociation of oleic acid in the membrane. The apparent pKa of oleic acid in a DPPC membrane was 8.8–9.4 ± 0.2, wherein oleic acid does not deprotonate at pH 5.8. More broadly, the deprotonation of oleic acid as a function of the pH is also relevant to non-biological applications such as stabilization of nanoparticles by oleic acids [48] and emulsion stabilization in lipid droplets [49], drug delivery systems, as well as food applications. The fluidization of saturated DPPC lipid membranes by oleic acid was apparent from the magnitude of adhesion between 7:3 DPPC-oleic acid membranes. The magnitude of adhesion was lower compared to the adhesion of gel phase DPPC membranes and was consistent with previously established value for adhesion between fluid phase PC membranes. The ability of oleic acid to interact with lipids and alter the interaction between membranes is important especially in the latest field of molecular therapy for the pharmaceutical industry. Oleic acid is able to regulate the localization and activity of membrane proteins in lipid rafts, which is important due to membrane proteins ability to control cell signaling and gene expression. In summary, the findings clearly demonstrate that oleic acid interacts favorably with saturated DPPC and that oleic acid's degree of deprotonation can be tailored by the solution pH enabling the interaction between oleic acid containing membranes, which have not previously studied, to be controlled. Additional studies, such as high resolution X-ray and neutron scattering measurements and other techniques, would help further characterize how oleic acid alters membrane structure and properties.

Conflict of interest

The authors declare no competing financial interest.

Transparency document

The Transparency document associated with this article can be found, in the online version.

Acknowledgement

This work was primarily supported by the NSF chemistry division through grant CHE-1413745. We thank Joao Ventrici for the assistance with atomic force microscopy. Keishi Suga expresses his gratitude for Engineering Science Young Researcher Dispatch Program and Multidisciplinary Research Laboratory System of Osaka University.

Supplementary Data

Appendix A: Force-distance profiles of 7:3 DPPC-oleic data containing multiple data sets for each experimental condition. *Appendix B*:

Equations and sample calculations for apparent pKa of oleic acid from SFA data. Supplementary data associated with this article can be found in the online version, at http://dx.doi.org/10.1016/j.bbamem.2016.11.001.

References

[1] W.E. Hardman, (n−3) Fatty acids and cancer therapy, J. Nutr. 134 (2004) 3427 s–3430 s.
[2] A. Pagnan, R. Corrocher, G.B. Ambrosio, S. Ferrari, P. Guarini, D. Piccolo, A. Opportuno, A. Bassi, O. Olivieri, G. Baggio, Effects of an olive-oil-rich diet on erythrocyte-membrane lipid-composition and cation-transport systems, Clin. Sci. 76 (1989) 87–93.
[3] A. Kagan, B.R. Harris, W. Winkelstein, K.G. Johnson, H. Kato, S.L. Syme, G.G. Rhoads, M.L. Gay, M.Z. Nichaman, H.B. Hamilton, J. Tillotson, Epidemiologic studies of coronary heart-disease and stroke in Japanese men living in Japan, Hawaii and California - demographic, physical, dietary and biochemical characteristics, J. Chronic Dis. 27 (1974) 345–364.
[4] L.H. Kushi, R.A. Lew, F.J. Stare, C.R. Ellison, M. Ellozy, G. Bourke, L. Daly, I. Graham, N. Hickey, R. Mulcahy, J. Kevaney, Diet and 20-year mortality from coronary heart-disease - the Ireland-Boston Diet Heart Study, N. Engl. J. Med. 312 (1985) 811–818.
[5] F.B. Hu, M.J. Stampfer, J.E. Manson, E. Rimm, G.A. Colditz, B.A. Rosner, C.H. Hennekens, W.C. Willett, Dietary fat intake and the risk of coronary heart disease in women, N. Engl. J. Med. 337 (1997) 1491–1499.
[6] M. Delorgeril, S. Renaud, N. Mamelle, P. Salen, J.L. Martin, I. Monjaud, J. Guidollet, P. Touboul, J. Delaye, Mediterranean alpha-linolenic acid-rich diet in secondary prevention of coronary heart-disease, Lancet 343 (1994) 1454–1459.
[7] J. Hartweg, R. Perera, V. Montori, S. Dinneen, H.A.W. Neil, A. Farmer, Omega-3 polyunsaturated fatty acids (PUFA) for type 2 diabetes mellitus, Cochrane Database Syst. Rev. (2008).
[8] W.S. Lim, J.K. Gammack, J. Van Niekerk, A.D. Dangour, Omega 3 fatty acid for the prevention of dementia, Cochrane Database Syst. Rev. (2006).
[9] C. McKarney, M. Everard, T. N'Diaye, Omega-3 fatty acids (from fish oils) for cystic fibrosis, Cochrane Database Syst. Rev. (2007).
[10] S. Dayton, M.L. Pearce, S. Hashimoto, W.J. Dixon, U. Tomiyasu, A controlled clinical trial of a diet high in unsaturated fat in preventing complications of atherosclerosis, Circulation 40 (1969) (Ii1-&).
[11] M. Miettinen, O. Turpeinen, M.J. Karvonen, M. Pekkarinen, E. Paavilainen, R. Elosuo, Dietary prevention of coronary heart-disease in women - the Finnish Mental-Hospital Study, Int. J. Epidemiol. 12 (1983) 17–25.
[12] A.S. Dontas, N.S. Zerefos, D.B. Panagiotakos, D.A. Valis, Mediterranean diet and prevention of coronary heart disease in the elderly, Clin. Interv. Aging 2 (2007) 109–115.
[13] P. Nestel, P. Clifton, D. Colquhoun, M. Noakes, T.A. Mori, D. Sullivan, B. Thomas, Indications for omega-3 long chain polyunsaturated fatty acid in the prevention and treatment of cardiovascular disease, Heart Lung Circ. 24 (2015) 769–779.
[14] J.R. Usher, R.M. Epand, D. Papahadjopoulos, Effect of free fatty-acids on thermotropic phase-transition of dimyristoyl glycerophosphocholine, Chem. Phys. Lipids 22 (1978) 245–253.
[15] R.D. Klausner, A.M. Kleinfeld, R.L. Hoover, M.J. Karnovsky, Lipid domains in membranes - evidence derived from structural perturbations induced by free fatty-acids and lifetime heterogeneity analysis, J. Biol. Chem. 255 (1980) 1286–1295.
[16] N. Muranushi, N. Takagi, S. Muranishi, H. Sezaki, Effect of fatty-acids and monoglycerides on permeability of lipid bilayer, Chem. Phys. Lipids 28 (1981) 269–279.
[17] M. Ibarguren, D.J. Lopez, P.V. Escriba, The effect of natural and synthetic fatty acids on membrane structure, microdomain organization, cellular functions and human health, Bba-Biomembranes 1838 (2014) 1518–1528.
[18] S.S. Funari, F. Barcelo, P.V. Escriba, Effects of oleic acid and its congeners, elaidic and stearic acids, on the structural properties of phosphatidylethanolamine membranes, J. Lipid Res. 44 (2003) 567–575.
[19] A.M.G. da Silva, R.I.S. Romao, Mixed monolayers involving DPPC, DODAB and oleic acid and their interaction with nicotinic acid at the air-water interface, Chem. Phys. Lipids 137 (2005) 62–76.
[20] T. Inoue, S. Yanagihara, Y. Misono, M. Suzuki, Effect of fatty acids on phase behavior of hydrated dipalmitoylphosphatidylcholine bilayer: saturated versus unsaturated fatty acids, Chem. Phys. Lipids 109 (2001) 117–133.
[21] Y. Onuki, M. Morishita, Y. Chiba, S. Tokiwa, K. Takayama, Docosapentaenoic acid and eicosapentaenoic acid induce changes in the physical properties of a lipid bilayer model membrane, Chem. Pharm. Bull. 54 (2006) 68–71.
[22] J. Cerezo, J. Zuniga, A. Bastida, A. Requena, J.P. Ceron-Carrasco, Atomistic molecular dynamics simulations of the interactions of oleic and 2-hydroxyoleic acids with phosphatidylcholine bilayers, J. Phys. Chem. B 115 (2011) 11727–11738.
[23] D.P. Cistola, J.A. Hamilton, D. Jackson, D.M. Small, Ionization and phase-behavior of fatty-acids in water - application of the Gibbs phase rule, Biochemistry-Us 27 (1988) 1881–1888.
[24] S. Salentinig, L. Sagalowicz, O. Glatter, Self-assembled structures and pK(a) value of oleic acid in systems of biological relevance, Langmuir 26 (2010) 11670–11679.
[25] S. Trier, J.R. Henriksen, T.L. Andresen, Membrane fusion of pH-sensitive liposomes - a quantitative study using giant unilamellar vesicles, Soft Matter 7 (2011) 9027–9034.
[26] J.R. Kanicky, D.O. Shah, Effect of degree, type, and position of unsaturation on the pK(a) of long-chain fatty acids, J. Colloid Interface Sci. 256 (2002) 201–207.
[27] K. Suga, T. Yokoi, D. Kondo, K. Hayashi, S. Morita, Y. Okamoto, T. Shimanouchi, H. Umakoshi, Systematical characterization of phase behaviors and membrane properties of fatty acid/didecyldimethylammonium bromide vesicles, Langmuir 30 (2014) 12721–12728.
[28] N. Duzgunes, R.M. Straubinger, P.A. Baldwin, D.S. Friend, D. Papahadjopoulos, Proton-induced fusion of oleic acid phosphatidylethanolamine liposomes, Biochemistry-Us 24 (1985) 3091–3098.
[29] N. Duzgunes, S. Nir, Mechanisms and kinetics of liposome-cell interactions, Adv. Drug Deliv. Rev. 40 (1999) 3–18.
[30] J.N. Israelachvili, G.E. Adams, Measurement of forces between 2 mica surfaces in aqueous-electrolyte solutions in range 0–100 Nm, J. Chem. Soc. Faraday Trans. 1 74 (1978) (975-&).
[31] J. Kurniawan, N.N. Yin, G.Y. Liu, T.L. Kuhl, Interaction forces between ternary lipid bilayers containing cholesterol, Langmuir 30 (2014) 4997–5004.
[32] D.F. Kienle, J.V. de Souza, E.B. Watkins, T.L. Kuhl, Thickness and refractive index of DPPC and DPPE monolayers by multiple-beam interferometry, Anal. Bioanal. Chem. 406 (2014) 4725–4733.
[33] J. Kurniawan, T.L. Kuhl, Characterization of solid-supported dipalmitoylphosphatidylcholine membranes containing cholesterol, Langmuir 31 (2015) 2527–2532.
[34] J. Marra, J. Israelachvili, Direct measurements of forces between phosphatidylcholine and phosphatidylethanolamine bilayers in aqueous-electrolyte solutions, Biochemistry-Us 24 (1985) 4608–4618.
[35] J.N. Israelachvili, Thin-film studies using multiple-beam interferometry, J. Colloid Interface Sci. 44 (1973) 259–272.
[36] G.L. Gaines, Insoluble Monolayers at Liquid-gas Interfaces, Interscience Publishers, New York, 1966.
[37] F.C. Goodrich, Molecular interaction in mixed monolayers, Proceedings of the Second International Congress of Surface Activity, vol. 15, Butterworth, London 1957, p. 85.
[38] B. Dejanovic, V. Noethig-Laslo, M. Sentjurc, P. Walde, On the surface properties of oleate micelles and oleic acid/oleate vesicles studied by spin labeling, Chem. Phys. Lipids 164 (2011) 83–88.
[39] E.B. Watkins, C.E. Miller, D.J. Mulder, T.L. Kuhl, J. Majewski, Structure and orientational texture of self-organizing lipid bilayers, Phys. Rev. Lett. 102 (2009).
[40] Y. Onuki, C. Hagiwara, K. Sugibayashi, K. Takayama, Specific effect of polyunsaturated fatty acids on the cholesterol-poor membrane domain in a model membrane, Chem. Pharm. Bull. 56 (2008) 1103–1109.
[41] C.A. Helm, J.N. Israelachvili, P.M. Mcguiggan, Molecular mechanisms and forces involved in the adhesion and fusion of amphiphilic bilayers, Science 246 (1989) 919–922.
[42] H. Fukuda, A. Goto, H. Yoshioka, R. Goto, K. Morigaki, P. Walde, Electron spin resonance study of the pH-induced transformation of micelles to vesicles in an aqueous oleic acid/oleate system, Langmuir 17 (2001) 4223–4231.
[43] J.J. Janke, W.F.D. Bennett, D.P. Tieleman, Oleic acid phase behavior from molecular dynamics simulations, Langmuir 30 (2014) 10661–10667.
[44] S.D. Kramer, C. JakitsDeiser, H. WunderliAllenspach, Free fatty acids cause pH-dependent changes in drug-lipid membrane interactions around physiological pH, Pharm. Res. 14 (1997) 827–832.
[45] J.R. Kanicky, D.O. Shah, Effect of premicellar aggregation on the pK(a) of fatty acid soap solutions, Langmuir 19 (2003) 2034–2038.
[46] Y. Onuki, Y. Obata, K. Kawano, H. Sano, R. Matsumoto, Y. Hayashi, K. Takayama, Membrane microdomain structures of liposomes and their contribution to the cellular uptake efficiency into HeLa cells, Mol. Pharm. 13 (2016) 369–378.
[47] S. Teres, G. Barcelo-Coblijn, M. Benet, R. Alvarez, R. Bressani, J.E. Halver, P.V. Escriba, Oleic acid content is responsible for the reduction in blood pressure induced by olive oil, Proc. Natl. Acad. Sci. U. S. A. 105 (2008) 13811–13816.
[48] C.L. Nistor, R. Ianchis, M. Ghiurea, C.A. Nicolae, C.I. Spataru, D.C. Culita, J.P. Cusu, V. Fruth, F. Oancea, D. Donescu, Aqueous dispersions of silica stabilized with oleic acid obtained by green chemistry, Nanomaterials-Basel 6 (2016).
[49] A.R. Thiam, R.V. Farese, T.C. Walther, The biophysics and cell biology of lipid droplets, Nat. Rev. Mol. Cell Biol. 14 (2013) 775–786.